Fatigue Life Prediction of Titanium Implants with Titanium Dioxide Surface

Stepan Major, Vladimír Kocour and Jan Bryscejn

***Abstract*—**Most of mechanical components in the engineering are frequently subjected to multi-axial loading, which also applies to medical engineering. The cyclic-loading can lead to sudden fatigue failure. In present work the fatigue life of cylindrical titanium components of dental implants made from titanium alloys 6Al-4V ELI and 6Al-7Nb were studied. Contrary to surface treatments used in industry, the main goal of titanium dioxide deposition is to improve implants biocompatibility. The effect of surface treatment on fatigue life of implant was tested experimentally. Two sets of experimental samples differed in surface layer thickness, so that its influence can be compared. Its fatigue behaviour was studied and predictive models were tested. Seventeenth different models were applied and analysed in order to obtain the best way to predict fatigue life of implant. Two different types of implants were tested. First type of implant uses abutment screw to fix the crown. This type has four parts. Second type of dental replacement has only three components. This type utilizes abutment polygonal thorn to fix the crown. Experiments show that, the effect of titanium dioxide surfaces on implants mechanical properties is considered negligible. Therefore implants fatigue life is not dependent on dioxide layer thickness. The Gonçalves- Araujo- Mamiya criterion was found the best in implants fatigue prediction. The prediction of fatigue life of polygonal thorn is more complicated, so its prediction is gives inferior results contrary to the first type of implant.

***Keywords*—**Fatigue testing, Bending-torsion loading, Titanium dioxide, Biocompatibile surface, Dental replacement, Abutment screw

S. Major studied at the Brno University of Technology. He was working at the Institute of Theoretical and Applied Mechanics, Academy Science of Czech Republic, Prague. He was working at the Charles Univestity of Prague, The Faculty of Medicine, The Institute of Medical Physics and Engineering. S. Major is working at the University of Hradec Králové. (corresponding adress: University of Hradec Králové, Faculty of Education, Department of Technical Education. Hradec Králové, Rokitanského 62, Hradec Králové III, 500 03, Czech Republic, e-mail: s.major@ seznam.cz).

V. Kocour studied at the university Palackého Univesity in Olomouc, Faculty of Natural Science, Department of Applied of Physics and Metrology and he also studied at the Department of Optics and Optoelectronics. V. Kocour was also working at the at the Institute of Theoretical and Applied Mechanics, Department of Optical. V. Kocour was studied at the Czech Technical University Prague Faculty of Transportation. V. Kocour was also working at the Faculty of Mechanical Engineering of Czech Technical University Prague. He was researcher at Department of Measuring Techniques, Instrumentation and Metrology of this fakulty. Vladimír Kocour was taught mathematics at the Czech Technical University. Vladimír Kocour is specialist in the stereogrammetry and optical methods used in metalography and material research. The full adress o Faculty of Transportation, Czech Technical University, Zikova 1903/ 4 Prague, Czech Republic, (e-mail: V.Kocour@seznam.cz).

J. Bryscejn is working at The Theoretical and Applied Mechanics, Academy of Science, 190 00 Prague 9, Prosecká 809/76, (e-mail: Bryscejn@itam.go.com).

I. Introduction

EXPERINCE from the operation of many devices shows well that components subjected to the repeated loading will fail after a certain number of cycles. This will happen even in the case that loading amplitude is deep below ultimate tensile stress, respectively below yield stress. The fatigue degradation can be described as progressive and localized structural damage, this process caused significant damage in all areas of human activity [1] - [16]. Microscopic cracks will begin to form at the surface when the local value of above a certain threshold. This happens in places where the stress concentrators are present, i.e. in the corners and at the sharp edges or in places where material defects occur. These material defects can be often connected with fault thermal treatment or surface deposition. When local crack was generated, it will be growing and after some time will reach a critical size, and the structure will suddenly fracture.

As has already been said, the nominal maximum stress values are less than the yield stress limit of the metals. Fatigue failure occurs when a material is repeatedly subjected to external forces. This loading force is not necessarily described by periodic functions, i.e loading is not described by periodic function such as sine function and others.

An example of such non-periodic loading can be a dental implant [7], [14]. The dental implant consists of three or four main parts [7]. These components are: ceramic crown that is attached to the thorn or abutment screw and cylindrical housing. This abutment thorn or screw is inserted in the housing box, which is ingrown in the bone of the jaw. The abutment thorn has shape of conical thread or polygonal prism. The housing box (often called fixture) has internal cavity which serves to fasten the bolt or polygonal horn. This cavity has an internal thread or its cross-section is polygonal in the case of using polygonal thorn. Similar component as housing box in the jaw is often part of ceramic crown and this component serve to fast the thorn and the crown. It should be recounted, that most often solution is based on combination both approaches. The bottom section of thorn is a screw and its upper section is polygon (this section is mostly shorter than bottom section of thorn, see Fig.1). In some cases the abutment is another part of assembly. The abutment can be straight (this is a common form) or angled. An angled abutment is used for replacement of aslant growing teeth in the case that the implant must hold same slope as surrounding teeth.

In this article, the biological causes of the implant failure are not analyzed. Therefore, here is only a brief mention about reasons for the body rejection of implant as a foreign body. This process can be associated with various inflammations and other diseases [8], [9], [16]. This paper is devout only to mechanical causes of the implant failure, respectively to fatigue failure of a threaded or thorn caused by repeated forces. The thorn with thread can be considered as an example of cylindrical or conical sample with notch under bending-torsion loading.

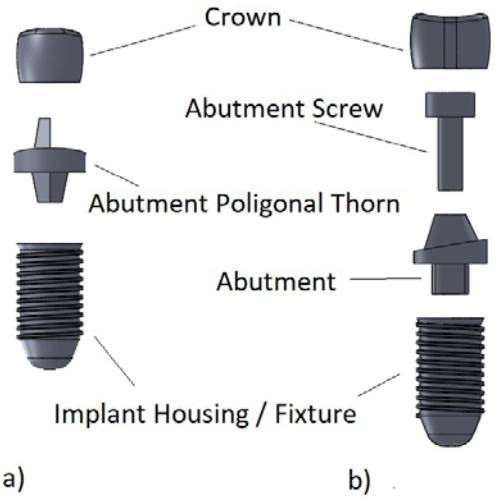

Fig. 1 Dental implants: (a) Implant with abutment thorn; (b) Implant with abutment and abutment screw.

II. Material of Implants

Majority of metal components used in dental implantology as well in medical engineering generally [7], [8], [9], [16] are manufactured from titanium alloys. Arguably, the most appropriate titanium alloys used in medicine are 6Al-4V ELI alloy and 6Al-7Nb alloy. The abbreviation ELI in denomination of the first alloy means Extra-Low Interstitials. Thus, titanium alloy 6Al-4V ELI is characterized by very low content of interstitial atoms. The main reason for reduce the concentration of interstitial atoms is that these atoms diffuse in the body. The interstitial atoms of vanadium are considered as harmful and carcinogen or cytotoxic.

The titanium alloy 6Al-4V ELI (ASTM standard: Grade 23 alloy) is very close to the titanium alloy 6Al-4V (ASTM standard: Grade 5 alloy), which is intended for industry and its mechanical properties are practically the same. The mechanical properties of titanium alloy 6Al-4V ELI are: Elastic modulus E = 113.8 MPa, ultimate strength $\sigma_u = 893$ MPa, yield stress $\sigma_y = 827$ MPa, crack growth properties are characterised by constants $C = 7.8 \cdot 10^{-14}$ and $m = 4.9$. These two constant are known from the Paris-Erdogan law. Crack growth properties were measured according to ASTM E647 [7], [8], [9], [18]. Due to the small dimensions of the implant, only first third of the stress curve was used obtained from this measurement was used for determination of stress crack growth parameters C and m. These values are therefore somewhat higher, than in the case of parameters whose values are determined from the entire loading curve. Because these values are higher than the values obtained from the entire curve, it is likely that the fatigue life will be slightly underestimated, i.e reability of design will be increased.

The titanium alloy 6Al-7Nb (ASTM standard: ASTM F 1295) was especially developed for medical use as alternative for 6Al-4V alloy. The mechanical properties of titanium alloy 6Al-4V ELI are: Elastic modulus E = 112 MPa, ultimate strength $\sigma_u = 895$ MPa, yield stress $\sigma_y = 819$ MPa, crack growth properties are characterised by constants $C = 6.4 \cdot 10^{-13}$ and $m = 8.2$.

III. Surface Treatment of Implants

One of the most common ways to improve components resistance to the external influences is modification of components surface. By changing surface layer properties of machinery parts it is possible to increase both corrosion resistance and their load-capacity. In case of medical engineering, the first task of surface layer deposition is upgrading of biocompatibility [7], [8], [9], [16], [19].The metallic alloy of which dental replacement is made, can release harmful particles in the patient body. Release of these particles can be explained by corrosion. This corrosion is caused by implants contact with body fluids. Another important factor in implants failure is deposition of biological sediments on the implant surface. Therefore, self-cleaning is one of the most important properties of biocompatible surfaces.

The preferred surface treatment is titanium dioxide deposition [7], [8], [16], [19], [20]. The titanium dioxide surface is an example of nano-surface and its self-cleaning feature significantly increases the likelihood, that the implant will be accepted by the human body.

In medical engineering ion-beam-assisted sputtering deposition technique has been used to deposit thick and dense titanium dioxide films on titanium alloys and stainless steel surfaces [20]. The ion-beam-assisted sputtering deposition is combination of ion implantation with simultaneous sputtering or another physical vapour deposition technique. Configuration with sputter deposition is preferred. Sputtering is a physical vapour deposition, this technique involves ejecting material from “target” that is the source of source onto a “substrate”. In the case of studied implants the distance between the target and the substrate was set at 15 cm and the base pressure in the plasma chamber was 0,01. Titanium content in target was 99.99%. This target was sputtered with plasma beam characterized by specific energy 14 W.cm^{-2}. The content of argon in the plasma beam was 99.99% and reactive oxygen was introduced between the plasma and the substrate. An appropriate selection of the oxygen flow was required. For this work, we prepared samples at temperature 400 °C and two

deposition times, corresponding to equivalent film thicknesses of 5 nm and 20 nm. The deposition rates were determined by using a quartz crystal located in the deposition chamber near the substrate. The parameters of deposition process are same for both titanium alloys (6Al-4V ELI and 6Al-7Nb) used in the study.

Titanium 6Al-4V alloy is generally considered as a standard material when evaluating the fatigue resistance. However, the mechanical response of this alloy is extremely sensitive to prior thermo-mechanical processing [20]. The changes in the β grain size, the ratio of primary α phase transformed to β phase, the α grain size and the α/β morphologies, all this characteristics have grate impact on fatigue performance and mechanical properties of final product. Particularly high-cycle fatigue lifetime is heavily influenced. For example, maximum fracture toughness and fatigue crack growth resistance is achieved when Widmanstätten microstructure was achieved during heat treatment (annealing) [20]. In this case annealing is resulting β recrystallization. However, Widmanstätten microstructure leads to decline of fatigue resistance in the high cycle fatigue [17].

Therefore, specimens used in this study were processed to achieve development of a bi-modal primary α plus transformed β microstructure. In this manner probability of fatigue crack initiation was reduced [20]. In the case titanium alloy 6Al-7Nb is the effect of heat treatment less significant than in the case of 6Al-4V alloy.

The effect of dioxide surface on the fatigue resistance of implant is disputable. With regard to it and intensive cyclic loading of dental implant, it is necessarily study this problem.

IV. Testing of Abutment Screw

The geometry of experimental sample is based on standard dental implant. The testing sample used different type of crown. This crown was made from steel. The testing machine can be described as rotating plate with holes and base with implant holder. These two plates are alternately in the opposite direction. Alternating impact forces caused bending of implant. The implant is fixed on the base plate of testing machine, schematic view is shown on Fig. 2. The testing device is constructed like that mutual inclination of axes of both plates is changeable. The size of bending forces acting on sample is set by inclination of these two axes. The size of torsion loading (i.e forces which act on the circumference of the sample) is set according to the position of implant on the base plate. The fixed position which corresponds to the position of the lowest point of the notch on the top plate caused zero value of torsion forces. Frequency of loading is changeable by microcontroller.

This solution allows control the intensity of the impact forces. The experiments were performed on four sets of specimen: (1) specimens with screw and titanium dioxide surface layer 5 nm; (2) specimens with screw and titanium dioxide surface layer 20 nm; (3) specimens with polygonal thorn and titanium dioxide surface layer 5 nm; (4) specimens with polygonal thorn and titanium dioxide surface layer 20 nm. Experimental sets (1) and (2) were performed on 15 specimens each. Experimental sets (3) and (4) had 10 and 8 sample respectively. The loading the implant can be described as effect of two external forces: first force bends specimen and the second force cased twist of specimen. The implant, respectively the abutment screw or thorn is under bending-torsion loading. However, the bending forces prevail over torsion forces. The loading can be characterized by ratio between burdening forces or even more appropriately between stress amplitudes r_L caused by this forces. This ratio can be defined as $r_L = \tau_a / (\tau_a + \sigma_a)$, where τ_a is amplitude of stress caused by torsion and σ_a is amplitude of stress caused by bending forces. In this test the value of ratio r_L is about 0.2. The fatigue test was performed to final rupture of specimen. The experiments were performed at the room temperature. The fatigue life N_f of investigated specimens was in the order from 10^3 to 10^5 cycles. The fatigue crack generated in the region of maximal value of stress/strain. In the case of abutment screw, the fatigue crack originated on the bottom of thread. If the polygonal abutment thorn is used, the fatigue crack occurred on thorns tapering.

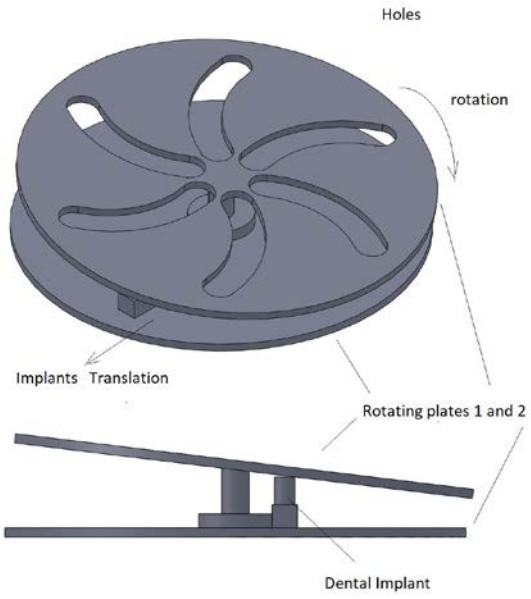

Fig.2 Fatigue testing- Principle of test machine. The plates are rotating and the implant can be shifted partially.

V. Fatigue Life Prediction

In practice majority of mechanical components in engineering practise is subjected to the bi-axial or tri-axial loading [3], [6], [21] - [23], eventually even more complicated cases. In general, the multi-axial loading can be described as combination of simple loading modes such as, torsion, bending or tension. This simple loading modes or forces could be

described by mutually independent functions. These functions are often time dependent components of stress tensor. When the individual components of stress tensor are in-phase during the loading, the fatigue life is usually shorter than in case of out-of-phase loading [3], [5].

In most industrial laboratories, there are only basic fatigue testing machines available. These basic machines does not allow multi-axial test. Therefore, one of the most difficult tasks in fatigue fracture simulation is to translate the information gathered from uni-axial fatigue tests on engineering materials into applications involving complex states of cyclic stress-strain conditions.

Many approaches have been proposed for prediction of multi-axial fatigue life prediction. Fatigue life prediction is often based by this approach: (1) The stress (respectively strain) state of component under loading is described by its location in stress-strain space; (2) This space is divided in two parts. Boundary curve (in case of bi-axial loading) or surface (universally in the case of multi-axial loading) divide stress space the stress space to the safe and the unsafe region [24], [25]. However, the function defining the division of the space is not yet established. In addition to a stress-based approach, equally strain based approach is used. Further, we encounter more complex approaches, such as approach based on Ilyushin space [26]. In addition to these methods, sometimes direct simulation of fatigue degradation is used, see [7] - [9]. However, this approach is not object of interest of this paper.

Let's start with the assumption, that the normal and shear stress components σ_a and τ_a, acting in a critical volume, control the fatigue life under combined bending-torsion loading. As far as, these components are known, the prediction of bi-axial fatigue life using data obtained by uni-axial tests is basically possible. As mentioned above, the stress space is divided to the safe and the unsafe parts by function or its value, which is called multi-axial fatigue criteria. The points bellow the boundary line lie in the safe region whereas the points above the line are in the unsafe region. The most general form of fatigue criteria can be written as an inequality:

$$a \cdot f(\tau_a) + b \cdot g(\sigma_a) \leq \sigma_c . \quad (1)$$

Where parameters a and b are limit values obtained from two uni-axial fatigue tests. Therefore, these two parameters corresponds to fatigue limit in fully reversed torsion τ_c and in tension σ_c). In some cases, the linear combination of shear stress τ_a and normal stress σ_a in Eq.1 can be replaced by a quadratic form.

In this paper seventeenth classical and advanced multi-axial criteria were used to predict the fatigue life of dental implants. This approach was used to assess the prediction quality: (1) If the load data of the left–hand side of Eq.1 (further referred as an abbreviation *LHS*) correspond the to experimentally determined fatigue limit (right-hand side *RHS* of the inequality Eq.1), the ideal state of equality should be achieved. The accuracy of the fatigue life prediction by means of multi-axial criteria can be expressed by the so-called error index *I*:

$$I = \left(\frac{LHS - RHS}{RHS} \right) \cdot 100\% . \quad (2)$$

The error index expresses a percentage of deviation from the real fatigue life. The ideal prediction leads to equality *LHS* = *RHS*, i.e. I = 0. The positive value of the error index means, that the criterion yields conservative results, i.e. the real fatigue life of implant is higher than that predicted by criterion and, therefore, the predicted number of cycles N_f to implant failure lies on the safe side of the boundary line.

VI. Criteria for Determination of Fatigue Life under Bi-axial Loading

Scope of this article does not allow a deeper analysis of all the compared criteria. Therefore, only some of the selected criteria are discussed in paper. Criteria discussed in the paper were selected to represent certain approaches to solving the problem. Criteria can be divided between classical and advanced. These approaches are also distinguished: quadratic form of classical criterion, critical plane approach and integral approach, criteria based on Ilyushin space. As the examples of classical fatigue criteria were tested criteria proposed by Gough and Pollard, McDiarmid, Matake or Kakun-Kawado criteria [3], [22] - [25]. As an example of integral approach were chosen two criteria: First Papadopoulos criteria and Keunmegna criteria. The criterion proposed by Gonçalves, Araujo and Mamiya is an example of criteria based on five-dimensional Ilyushin space. The Spagnoli criterion was chosen as an ilustration of criteria in the form of root of damage parameter. It is necessary to emphasize, that all criteria are adapted on the case notched specimen. Reason for this modification is a thread on the abutment. The thread is an example of notched specimen. These notches working as stress concentrators.

A. Gough-Pollard Criterion

The Gough - Pollard criterion is considered as the oldest multi-axial criteria, because it was proposed in the thirties of the twentieth century [24], [25]. These two authors suggested an empirical ellipse formula as a multi-axial fatigue criterion [5]. This relationship is suitable for ductile materials:

$$\left(\frac{A_{GP}\sigma_a}{\sigma_c} \right)^2 + \left(\frac{B_{GP}\tau_a}{\tau_c} \right)^2 \leq 1 . \quad (3)$$

Parameters A_{GP} and B_{GP} were obtained by comparison of the Wőhler curves for notched and smooth specimens. Both parameters are equal 1 for smooth specimens.

In the case of brittle materials was proposed used modified Gough - Pollard criteria. This criterion is considered as preferable sample with stress concentrators [5]:

$$\left(\frac{A_B\sigma_a}{\sigma_c}\right)^2\left(C_B\kappa_{GP}-1\right)+\frac{B_P\sigma_a}{\tau_c}\left(2-\kappa_{GP}\right)+\frac{A_B\sigma_a}{\tau_c}\le 1. \quad (4)$$

Where κ_{GP} is ratio of fatigue limit defined as $\kappa_{GP}=\sigma_C/\tau_C$ and parameters A_B, B_B and C_B were obtained by same approach as in the previous case. The ratio κ of fatigue limit is used in many other relationships in this text. Many of the following criterions used it or their first initial form used it, but afterwards this relationship has been improved many times. Newer criteria therefore work with a different shape than a simple fraction. That's the reason, why the ratio κ is marked by subscription derived from criterion name. This rule is used throughout this text.

B. McDiarmid Criterion

The McDiarmid [27] - [29] criterion is frequently used, because this criterion was implemented in commercial fatigue software such as MSC.Fatigue or FE-Fatigue. This author identifies damage parameter as maximum value of stress at the plane of maximum shear stress range. Damage is computed on this plane by combining the shear stress and normal stress. The McDiarmid criterion can be written according to convention defined by Eq. 1:

$$\frac{A_{MD}.\sigma_C.\tau_{a,\max}}{t_{A,B}}+\frac{B_{MD}\sigma_C}{2\sigma_U}\le C_{MD}\sigma_C. \quad (5)$$

Where, the σ_U is the ultimate strength. Parameters A_{MD}, B_{MD} and C_{MD} were obtained by comparison of the Wőhler curves for notched and smooth specimens. Subscript a mean amplitude and subscript max denotes maximum value of stress. The subscript A, B in this criterion represents choice between two distinct fatigue limits t_A a t_B. These two fatigue limits are corresponding to load conditions leading to cracks growing in two distinct directions:

1) in the first system the fatigue crack is growing parallel to the sample surface (A);
2) in the second case, the system is characterized by growth inwards from the surface, i.e. the crack growth in the plane perpendicular to the sample axis (B).

This distinction between two cracking systems is not usually defined. In the case of plane bending combined with torsion is generally fulfilled equality $t_{A,B}=\sigma_C$ [3], [21], [22], [29]. The loading region in which this criterion can be used reliably is defined by these inequalities:

$$\frac{\tau_c}{2}\le\tau_{a,mac}\le\tau_c,\quad 0\le\sigma_{n,\max}\le\sigma_U \quad (6)$$

C. Sines Criterion

This criterion is primarily used in the high cycle fatigue region [23], [30]. This criterion is defined as:

$$\sqrt{J_{2,a}}+\kappa_S\sigma_{h,m}\le\lambda_S, \quad (7)$$

where $J_{2,a}$ is the second invariant of stress tensor deviator and $\sigma_{h,m}$ is mean value of hydrostatic stress. Prameters κ_S and λ_S are obtined from two uniaxal test. These two uniaxial tests represent two limit cases: (1) symmetrical torsion and (2) bending loading. These two loading states are characterized by two extreme values of $J_{2,a}$ and hydrostatic stress: (1) $\sqrt{J_{2,a}}=\tau_c$ and $\sigma_{h,m}=0$ for symmetrical torsion; (2) $\sqrt{J_{2,a}}=\sigma_{c,R=0}$ and $\sigma_{h,m}=\sigma_{c,R=0}/3$ for bending loading. The value $\sigma_{c,R=0}$ represents the fatigue limit in the case of pulsative-bending, the loading force is growing from zero to amplitude and then decreasing to zero. Then, these two parameters can be expressed as:

$$\kappa_S=\frac{3\tau_C}{\sigma_{c,R=0}}-\sqrt{3},\quad \lambda_S=\tau_c. \quad (8)$$

In practice we often meet this approach to the problem: the value κ_S is modified using Goodman or Gerber relationship. The parameter can be written as:

$$\kappa_{S,Go}=\frac{\sqrt{3}\sigma_c}{\sigma_U},\ \kappa_{S,Ge}=\frac{\sqrt{3}\sigma_c\sigma_{c,R=0}}{\sigma_U}, \quad (9)$$

for Goodman relationship and Gerber relationship respectively.

D. Matake Criterion

Matake criterion belongs to criterions based on critical plane approach [3], [21] - [23],. Matake defined the critical plane according to the maximalization of $\tau_{a,\rho}$. The variable $\tau_{a,\rho}$ is maximal value of shear stress in common plane ρ. The critical plane is the plane in which it is valid

$$\tau_{a,\rho}=\max\left(\tau_{a,\rho}\right)\ge\tau_{a,\rho_I}. \quad (10)$$

This his applies to all planes that can be laid in this volume.

The Matake criterion can be written as an inequality:

$$C_M a_M\tau_{a,MSSR}+D_M b_M\sigma_{\max,MSSR}\le A_M\sigma_C. \quad (11)$$

Subscript MSSR by normal shear stress is abbreviation of Maximum Shear Stress (or Strain) Range. In same cases, variable $\sigma_{\max,MSSR}$ can be expressed as sum of amplite of normal stress and mean value of normal stress, i.e. it can be written as $\sigma_{\max,MSSR}=\sigma_{n,m}+\sigma_{n,a}$. Parameters a_M and b_M in this criteria are defined as $a_M=\kappa_M$ and $b_M=2-\kappa_M$. Variable κ_M is fatigue limits ratio $\kappa_M=\sigma_c/\tau_c$. Parameters A_M, C_M and D_M are equal to

1 for smooth specimen. These parameters were obtained by same manner as in the previous cases.

E. Findley Criterion

Also this criterion is belonging to the critical plane criterions [3], [31]. Contrary to the previous example, Findley chose a somewhat more complicated way of determining the critical plane. According to this author, the critical plane and also the stress concentration acting on this plane is defined using maximization of sum $\tau_{a,\rho}$ and $\kappa\sigma_\rho$. The stress $\tau_{a,\rho}$ and σ_ρ are maximal value of shear stress in common plane ρ and normal stress acting on this plane. The material parameter is:

$$\kappa_F = \sqrt{\frac{\frac{\tau_c}{\sigma_c} - \left(\frac{\tau_c}{\sigma_c}\right)^2 - \frac{1}{4}}{\left(\frac{\tau_c}{\sigma_c}\right)^2 - \frac{\tau_c}{\sigma_c}}}. \quad (12)$$

Then, the Findley criteria can be defined as:

$$\max(\tau_{a,\rho} + \kappa_F \sigma_\rho) \le \lambda_F, \quad (13)$$

where the material parameter λ_F is defined as a fraction:

$$\lambda_F = \frac{\sigma_c}{2\sqrt{\frac{\sigma_c}{\tau_c} - 1}}. \quad (14)$$

Parameter values σ_c and τ_c are obtained from uniaxial tests.

F. Crosland Criterion

Crosland published his criterion already before fifty years [3], [32]. His original criterion was intended for smooth specimen. This criterion is utilizing amplitude of the second invariant of stress tensor deviator. This deviator corresponds to the von Mises stress. If the notch is present, theoretically no adjustments are needed. Because, theoretically, we can assigned certain value of stress/strain tensor (or by its components) to each point in the implant should. Actually, some corrections are necessary. It should be recalled that the local value of stress, resp. stress intensity factor at the bottom of notch is depending on the notch geometry. The relation between geometry and stress at the bottom of the notch can described by $\propto 1/r^p$ [22]. The parameter r is radius on the bottom of the notch. It is obvious, that in the case of sharp edge the dangerous stress is growing steeply. The Crosland criteria modified for sample with V notch (characterized by acute angle between groove faces) can be written:

$$A_C a_C \sqrt{J_{2,a}} + B_C b_C \sigma_{H,a} \le \tau_c. \quad (15)$$

Parameters a_C and b_C can be obtained through the evaluation of the formulas at fatigue limits in torsion and tension or bending. The appropriate values of material parameters are $a_C = \kappa_C$ and $b_C = 3 - \sqrt{3}\kappa_C$. The parameters A_C, B_C are characterizing the influence of notch shape.

G. Kakun-Kawada Criterion

The Kakun-Kawada criteria [3], [22] can be written as:

$$a_K \sqrt{J_{2,a}} + b_K \sigma_{H,a} + c_K \sigma_{H,m} \le \tau_c. \quad (16)$$

Where, the $J_{2,a}$ is the second invariant of stress tensor deviator. The $\sigma_{H,a}$ and $\sigma_{H,m}$ are amplitude and mean value of hydrostatic stress. Parameters a_K, b_K and c_K are material parameters obtained from uni-axial fatigue test. The material parameters are definde as:

$$a_K \approx e^{1/r},\ b_K = B_K \kappa_{KK},\ c_K = C_K \mu_{KK}. \quad (17)$$

The parameters B_K, C_K and a_K are related to the notch geometry, their value is equal one in the case of smooth sample. The parameters κ_{KK} and μ_{KK} are defined as:

$$\kappa_{KK} = \frac{3\tau_c}{\sigma_c} - \sqrt{3},\ \mu_{KK} = \frac{3\tau_c}{\sigma_{c,0}} - \sqrt{3}. \quad (18)$$

If the Kakun-Kawada criterion is compared with criterion proposed by Crossland it is clear, that in some special cases both criterion are same.

H. Spagnoli Criterion

The Spagnoli criterion was chosen as an example of quadratic form of fatigue criteria [3], [33]. One of disadvantages of this criterion is fact that the majority of compared criterions is in linear form. So if we want to evaluate the quality of this criterion using the error index (2), we are probably making some inaccuracies. However, though this question has not yet been satisfactory answered, this procedure is commonly used.

Spagnoli criteria can be expressed in this form:

$$\sqrt{a_S \tau_{a,.\max}^2 + b_S \sigma_{n,\max}^2} \le \tau_c. \quad (19)$$

Where $\tau_{a,max}$ is amplitude of sheer stress in the plane of maximal sheer stress and $\sigma_{n,max}$ is maximal value of normal stress in the specimens volume. The pair of parameters was obtained from uniaxial fatigue tests. Also, the parameter on the right side of specimen was determined from simple uniaxial test. This parameter represents fatigue limit in torsion. The parameter is equal 1 for smooth steel specimen in the form of cylinder. However, in the case notched sample is about 1.3. Its value is strongly affected by the opening angle of the notch. The parameter b_S is equal to κ^2 in (18), and the requirement for

maximal damage in the plane is $\kappa < \sqrt{2}$. This condition is well fulfilled, becuse κ is 1.2× smaller for notched sample than for smooth specimens.

I. Papadopoulos Critical Plane Criterion

This criterion was proposed by Papadopoulos and in the following text, it will be referred to as PCP to distinguish it from a more familiar criterion based integral approach (i.e. this second criteria is utilizing average stresses in the sample elementary volume) and proposed by the same author. The PCP criterion was based on critical plane concept [3], [23], [34] - [36]. This criterion is given by inequality:

$$a_{PCP}\tau_{\chi} + b_{PCP}\sigma_{h,\max} \le \lambda_{PCP} \ . \tag{20}$$

The parameter τ_{χ} is mean value of shear stress amplitude calculated over all directions (defined by angles φ, ψ and χ) in critical plane, i.e in the plane of maximal damage. This variable can be calculated as:

$$\tau_{\chi} = \sqrt{\frac{1}{\pi}\int_{\chi=0}^{2\pi}\tau_a(\varphi,\psi,\chi)d\psi} \ . \tag{21}$$

The parameters a_{PCP} and b_{PCP} are obtained from relationships:

$$a_{PCP} = S\kappa_{PCP}, \quad b_{PCP} = B - C\kappa_{PCP} . \tag{22}$$

The parameters κ and λ are obtained from simple uniaxial tests. Its values are

$$\kappa_{PCP} = \frac{\tau_C}{\sigma_C}, \ \ \lambda_{PCP} = \tau_C . \tag{23).}$$

The assessment of parameters S, B and C is more complicated than previous. The value of parameter S can be described as $1 \le S \le 2$, the value 1 correspond to the smooth specimen. The parameters B and C have values $7/3 \le B \le 3$ (the higher one corresponding to the smooth sample) and $3/2 \le S \le 2$.

J. Dang Van Criterion

This criterion can be classified among criterions based on the microscopic approach. From a macroscopic point of view, the nucleation process of the fatigue crack can be considered as process that occurs in an elementary volume. This elementary volume is made up of one, at most, a few adjacent grains. Local values of stress in these metal grains can vary substantially from macroscopic values. This fact is can be explained in this way:

1) from microscopic point of view the material can not be considered as homogeneous;
2) these metal grains are randomly oriented, in small volume only a few grains are lying and the mechanical properties are depending on grain orientation, i.e. the material is not isotropic.

Dang Van defined its criterion as [3], [23], [37] - [39]:

$$\tau_{\max,a} + \kappa_{DV}\sigma_h \le \lambda_{DV} , \tag{24}$$

where κ_{DV} and λ are material constants and $\tau_{max,a}$ is amplitude of maximal sheer stress in elementary volume. The stress σ_h is hydrostatic stress defined simply as the average of the three normal stress components of any stress tensor $\sigma_h = (\sigma_{11} + \sigma_{22} + \sigma_{33})/3$. The parameters κ_{DV} and λ_{DV} are defined as:

$$\kappa_{DV} = \frac{\tau_C + \frac{\sigma_C}{2}}{\frac{\sigma_C}{3}}, \quad \lambda_{DV} = \tau_C . \tag{25}$$

In this form (23) is this criterion widely used in praxis, but this form some shortcomings, which limit its accuracy in the case of notched specimen. For this reason, the criterion was modified by correlation coefficients A_{DV} and B_{DV}. One of these coefficients takes into account ratio between sample diameter and the depth of notch, i.e. the sample taper. It is therefore a coefficient expressing the local increase of tension in the notched area. Second parameter B_{DV} takes into account the shape of notch $\propto 1/r^{p}$.

K. Keunmegna Integral Criterion

The Keunmegna integral criterion based on integral approach is one example of advenced stress based kriteria [40]. This criterion can be expressed as:

$$\sqrt{\int_{\varphi=0}^{2\pi}\int_{\psi=0}^{\pi}\frac{\phi(\tau_a,\sigma_a,\sigma_m)}{4\pi.Q_{Ke}}\sin\psi d\psi d\varphi} \le \sigma_c \ . \tag{26}$$

Where, φ and ψ are Euler angles between the global coordinate system and the examined plane. The subscript m denotes mean value of stress. The function $\phi(\tau_a,\sigma_a,\sigma_m)$ in Eq.8 can be written as:

$$\phi(\tau_a,\sigma_a,\sigma_m) = A_{Ke}a_{\kappa}\tau_a + B_{Ke}b_{\kappa}\sigma_a + D_{Ke}d_{\kappa}\sigma_m . \tag{27}$$

Parameters A_{Ke}, B_{Ke}, D_{Ke} and Q_{Ke} represents correlation of elevation of local stress value caused by cross-sectional reduction at the bottom of thread. These parameters are functions of the notch profile. Parameters a_{κ}, b_{κ} and c_{κ} are material parameters.

L. Papadopoulos Integral Criterion

The example of advanced stress based multi-axial criteria is Papadopoulos integral criterion [3], [23], [34], [35]. In Papadopoulos criterion based on integral approach are both input variables (shear stress and normal stress) integrated over all planes:

$$\sqrt{a_P\iiint T_a^2 d\chi\sin\psi d\psi d\varphi} + b_P\cdot\sigma_{H,\max} \le \sigma_c . \tag{28}$$

The variable $T_a = T_a(\varphi,\psi,\chi)$ is amplitude of resolved stress. Because, the resolved stress is function of Euler angles φ, ψ and χ, the amplitude of stress is identified by stress maximalization in all directions. The $\sigma_{H,,max}$ is maximum value of hydrostatic stress. The parameters a_P and b_P are defined as:

$$a_P = \frac{5\kappa_P^{\,2}}{8\pi^2},\ b_P = 3 - 3\kappa_P . \tag{29}$$

M. Gonçalves- Araujo- Mamiya Criterion

Criterion proposed by trio Brazilian authors Gonçalves, Araujo and Mamiya is considered as very effective [41]. This trio of authors assumes that the ultimate value of loading corresponds to valume of circumscribed ellipsoid in Ilyushin space proposed by Freites [26], [42]. The volume of this ellipsoid was expressed as:

$$f = \sqrt{\sum_{i=1}^{5} a_i^2}\ , \tag{30}$$

where a_i corresponds to the half-axis length which bounds stress trajectory in five-dimensional deviatoric space. In the specific case of sinusoidal loading, the problem will be significantly simplified. In this case we can write this equality:

$$\sqrt{\sum_{i=1}^{5} a_i^2} = \sqrt{\sum_{i=1}^{5} d_i^2}\ , \tag{31}$$

where d_i is distance between central point of ellipsoid and the surface of enveloping rectangular prism. This prism enveloped all points of stress trajectory. The calculation is realized for every existing enveloping rectangular prism in the five-dimensional space.

This criterion is utilizing a construction of minimum circumscribed ellipsoid over the load path in five-dimensional deviatoric Ilyushin space. This criterion exploit maximal value of main stress as second input. This criterion can be expressed as:

$$a_{GAM}\sqrt{\sum_{i=1}^{5} d_i^2} + b_{GAM}\sigma_{1,\max} \le \sigma_c\ , \tag{32}$$

where parameters d_i can be determined from minimum and maximum values of the transformed deviatoric stress tensor:

$$d_i = \frac{1}{2}\left(\max s_i(t) - \min s_i(t)\right), \tag{33}$$

The material parameters a_{GAM} and b_{GAM} are defined as:

$$a_{GAM} = \frac{\kappa_{GAM} - 1}{\sqrt{2}\left(1 - \frac{1}{\sqrt{3}}\right)}\ ,\quad b_{GAM} = \frac{\sqrt{3} - \kappa_{GAM}}{\sqrt{3} - 1}. \tag{34}$$

N. Zenner- Liu Criterion

This criterion is more complicated than previous. Above all, however, this criterion needs a larger number of input parameters than other criteria discussed in this paper [43] - [45]. This criterion can be written in this form:

$$\sqrt{\frac{1}{\pi}\int_{\varphi=0}^{2\pi}\int_{\psi=0}^{\pi}\left[a_{ZL}\tau_a^2 C_{ZL} + b_{ZL}\sigma_a^2 D_{ZL}\right]\sin\psi d\psi d\varphi} \le \lambda_{ZL}\ , \tag{35}$$

where τ_a and σ_a are sheer stress amplitude and normal stress amplitude. Variables C_{ZL} and D_{ZL} are used only for shortening and we can express them:

$$C_{ZL} = 1 + c_{ZL}\tau_m^2\ ,\ D_{ZL} = 1 + d_{ZL}\sigma_m^2\ . \tag{36}$$

The variables τ_m and σ_a are mean value of sheer stress and normal stress. The parameters a_{ZL}, b_{ZL}, c_{ZL} are d_{ZL} are defined by the following relationships:

$$a_{ZL} = \frac{3}{2}\left(3\kappa^2 - 4\right),\quad b_{ZL} = 3\left(3 - \kappa^2\right). \tag{37}$$

The following two relationships already use the results (38):

$$c_{ZL} = \frac{1}{a_{ZL}}\frac{28}{3\tau_{t,c_0}^{\,4}}\left[\lambda_{ZL}^{\,2} - \left(\frac{\kappa_{ZL}\tau_{t,c}}{2}\right)^2\right], \tag{39}$$

$$d_{ZL} = \frac{1}{b_{ZL}}\frac{28}{15\sigma_{T,c}}\left[\left(\frac{2\lambda_{ZL}}{\sigma_{T,c}}\right)^2 - \frac{4}{21}c_{ZL}a_{ZL}\left(\frac{\sigma_{T,c}}{2}\right)^2 - 1\right]. \tag{40}$$

From the above relationships, it is clear that the determination of the relevant parameters is very complicated. Some authors (Papadopoulos for example) strongly criticize this fact. The parameter λ_{ZL} on the right hand side of (35) is equal to fatigue limit in fully reversed push-pull $\sigma_{PP,c}$. The parameter $\kappa_{ZL} = \sigma_{PP,c}/\tau_c$ is ratio known from (4). Material parameters such as $\sigma_{T,c}$, $\tau_{t,c}$, $\sigma_{PP,c}$, $\tau_{-1,c}$ are obtained from uniaxial fatigue tests. Their meaning is fatigue limit in repeated tension, fatigue limit in repeated torsion, fully reversed push-pull and fatigue limit in fully reversed torsion. This means that, the uniaxial tests are carried out in two loading modes:

1) In firs case the loading force is growing from zero to its maximum and then drops to zero again. This is still repeated. This process can be described for example by $L(t) = L_a\sin(\omega.t) + L_a$, i.e if $\omega t = 3\pi/2$, the load $L(t) = 0$ N.
2) The second set of tests is fully reversed and the loading

force changes from L_a to $-L_a$.

O. Papuga Improved Criterion

This criterion was proposed by Papuga as improvement previous criterion. This criterion combined approaches proposed by Zenner, Liu with method proposed by Kenmeugne. The improved criterion can be expressed as:

$$\sqrt{\frac{1}{4\pi}\int_{\varphi=0}^{2\pi}\int_{\psi=0}^{\pi}\left[\frac{5\kappa_{Pap}^{\ 2}}{2}+K_{Pap}\lambda_{Pap}\right]\sin\psi d\psi d\varphi}\le\lambda_{Pap}. \quad (41)$$

The parameter on the right hand of (41) is $\lambda_{Pap}=\sigma_c$. The value of fatigue limit σ_c was obtained from uniaxial test. The parameter K_{Pap} can be expressed as:

$$K_{Pap}=\left(3-\kappa_{Pap}^{\ 2}\right)\left(\sigma_a+\kappa_{Pap}\sigma_m\right). \quad (42)$$

The fatigue ratio is defined as $\kappa_{Pap}=\sigma_C/\tau_C$, i.e. just like in the case of (4).

VII. Predictions Efficiency and Experimental Results

The Fig. 3 shows fatigue life curves and experimental points of sample failure. These curves were drawn according von Mises stress σ_M. It is obvious, that the specimens with abutment thorn show greater scattering in the graph, which generally reduces prediction effectiveness.

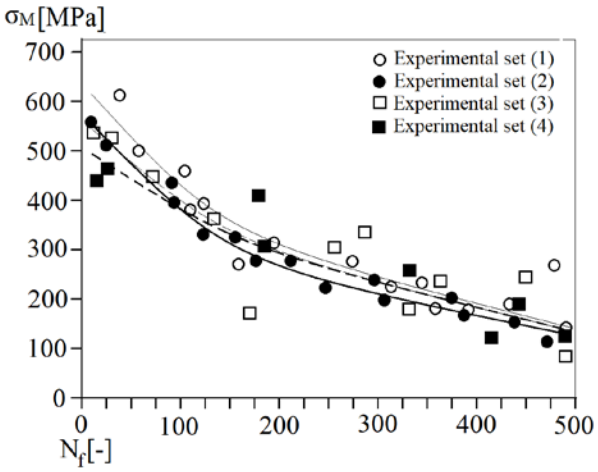

Fig. 3 Fatigue life curves and experimental points of sample failure. The specimens with surface layer thickness 20 nm are marked with black symbol and thick line. The specimens with surface layer thickness 5 nm are marked with empty symbol and thin line. The implants with abutment thorn are recognized by dash line and squares symbols. These curves were drawn according von Mises stress σ_M. The fatigue limit is expressed in 10^3 of cycles.

Samples with 20 nm thick surface layer have slightly smaller fatigue resistance than samples with 5 nm thick surface layer. Therefore, it can be said, that the titanium dioxide surface slightly reduces fatigue life, but this effect is negligible. However, the fatigue strength dramatically drops when the peak stress in the cycle reaches the strength of the TiO_2 particles. It is therefore necessary to spread the TiO_2 particles evenly over the surface.

The calculated error indexes are displayed for comparison in Table 1 and 2 for samples with surface layer 5 nm and Table 3 and 4 for surface layer 20 nm.

Table 1. Implant with abutment screw: *Average* I_{avr} and absolute average $I_{ABS,avr}$ values of error indexies – thickness of TiO_2 layer 5 nm. Abbreviations are described at the text.

	Error indexes [%]		Standard deviation
Abutment	Screw		
Criterion	I_{avr}	$I_{ABS,avr}$	*SD(I)*
GP	-5.83	9.21	3.5
GPBr	-1.36	8.78	5.2
F	-1.78	9.62	3.9
Ma	-0.21	7.32	3.2
MD	1.79	8.47	4.2
Sp	-1.45	8.03	3.3
PCP	-8.20	17.23	4.0
Mr	4.28	8.72	3.9
S	4.65	12.32	5.6
C	-3.47	8.63	4.9
KK	-2.49	8.65	3.6
DV	-1.55	8.95	4.7
PIA	-2.35	8.46	4.5
GAM	-1.05	7.93	3.3
Ke	-2.39	8.79	3.4
ZL	-3.99	12.35	7.2
Pap	-2.99	8.35	3.6

Table 2. Implant with abutment thorn: Average I_{avr} and absolute average $I_{ABS,avr}$ values of error indexies – thickness of TiO_2 layer 5 nm. Abbreviations are described at the text.

	Error indexes [%]		Standard deviation
Abutment	Thorn		
Criterion	I_{avr}	$I_{ABS,avr}$	*SD(I)*
GP	-7.43	12.25	5.8
GPBr	-3.63	21.49	5.0
F	-2.78	10.28	5.1
Ma	-1.79	9.68	5.4
MD	2.72	11.53	4.9
Sp	2.90	10.97	4.4
PCP	-7.03	16.65	4.7
Mr	3.76	11.72	4.7
S	13.65	17.25	5.9
C	1.93	12.11	4.8
KK	-2.63	13.57	4.9
DV	3.37	12.43	5.7
PIA	-1.98	10.98	5.1
GAM	-1.45	8.12	4.2
Ke	-3.11	9.93	5.8
ZL	5.21	17.83	6.3
Pap	3.21	11.38	5.6

The type of tested implant is always listed in the table, in the second row. For all studied criteria were calculated average

I_{avr} and absolute average $I_{ABS,avr}$ values of error indexies. Because the average value is not sufficient for statistical evaluation of presented measurement set, the quality of studied criterions was assessed using standard deviation *SD(I)*:

$$SD(I) = \sqrt{\frac{1}{N_S}\sum_{i=1}^{N_S}\left(I_i - I_{avr}\right)}, \quad (43)$$

where N_S is number of samples in experimental set.

Table 3. Implant with abutment screw: *Average* I_{avr} and absolute average $I_{ABS,avr}$ values of error indexies – thickness of TiO_2 layer 20 nm. Abbreviations are described at the text.

	Error indexes [%]		Standard deviation
Abutment	Screw		
Criterion	I_{avr}	$I_{ABS,avr}$	*SD(I)*
GP	-5.32	8.96	2.8
GPBr	-1.36	8.78	3.6
F	-1.42	8.63	3.4
Ma	-0.83	7.16	3.1
MD	1.56	8.13	2.9
Sp	-0.89	8.69	3.1
PCP	-8.20	9.21	4.9
Mr	3.87	8.43	3.7
S	3.98	9.72	3.2
C	-2.76	8.31	3.4
KK	-3.09	7.99	2.9
DV	-2.11	8.15	3.6
PIA	-2.38	8.28	3.9
GAM	-1.27	7.65	3.0
Ke	-2.79	8. 61	5.0
ZL	-9.07	13.34	5.1
Pap	-3.07	7.98	3.8

Table 4. Implant with abutment thorn: Average I_{avr} and absolute average $I_{ABS,avr}$ values of error indexies – thickness of TiO_2 layer 20 nm. Abbreviations are described at the text.

	Error indexes [%]		Standart deviation
Abutment	Thorn		
Criterion	I_{avr}	$I_{ABS,avr}$	*SD(I)*
GP	-8.01	13.05	6.7
GPBr	-7.37	22.16	4.6
F	-1.99	9.86	4.7
Ma	-2.31	9.92	5.5
MD	3.48	13.68	5.3
Sp	3.32	13.76	4.7
PCP	-4.06	12.35	5.6
Mr	-4.63	12.62	5.9
S	13.42	15.23	5.6
C	1.32	9.72	5.9
KK	-3.27	11.72	5.0
DV	-2.63	13.57	5.2
PIA	-2.19	9.32	5.8
GAM	-1.48	8.56	4.3
Ke	-3.78	10.39	5.6
ZL	4.12	12.58	7.9
Pap	3.46	11.37	3.9

Meaning of Abbreviations used in the tables: Gough-Pollard GP; Gough-Pollard for brittle materials GPBr; Findley F; Matake Ma; Marin Mr; Sines S; Crosland C; Dang Van DV; McDiarmid MD; Spagnoli Sp; Gonçalves-Araujo-Mamiya GAM; Kakun-Kawado KK; Keunmegna Ke; Zenner-Liu ZL; Papadopoulos Integral approach PIA; Papadopoulos Critiacal Plane approach PCP; Papuga Pap.

The comparison of multi-axial criteria data revealed that the Matake criterion was the most successful in the fatigue life prediction for surface abutment screw with 5 nm surface layer. Its average erorr index is I_{avr} = -0.21 and standard deviation *SD(I)* = 3.2, see Table 1. However, the results were much worse in the case implants with abutment thorn (I_{avr} = -1.79, *SD(I)* = 5.4). The Gonçalves, Araujo and Mamiya criterion gives bests results in this case of implants with the thorn erorr index is I_{avr} = -1.45 and standard deviation *SD(I)* = 4.2, see Table 2. Also, this criterion gives good results for standard implant with bolt. This criterion gives very good results in the case of thicker surface layer: I_{avr} = -1.27 for screw abutment and standard deviation *SD(I)* = 3.0, see Table 3. In the case of abutment thorn and thick surface layer gives these results: I_{avr} = -1.48 and *SD(I)* = 4.3, see Table 4. Generally, the prediction of fatigue life was much more difficult in the case of thorn abutment, as is evident from the worse results in this case. These results would certainly deserve a more detailed statistical analysis but, the scope of work does not allow this.

If we consider the complex of fatigue prediction criteria and their possible use in professional software for industrial computing, Gonçalves, Araujo and Mamiya criterion can be considered a suitable for utilization in industry [16].

VIII. Conclusion

The application of titanium dioxide surface leads to small decrease in the fatigue resistance in the low cycle region. So there it is not reason to use resign on this treatment, because there is greater risk for implant failure from biological reason than from the fatigue loading.

The comparison of multiaxial criteria revealed that the Gonçalves, Araujo and Mamiya and Matake criterion are the most successful in the fatigue life prediction of both type of implant. The average value of the error index (taking into account the sign) is the lowest one (I_{avr} = - 1.05). Also the average absolute value of the error index $I_{ABS,avr} = 7.93\%$ is very good. Also its standard deviation *SD(I)* = 3.3 is satisfatory.

Acknowledgment

This project was prepared by financial support J & J & Co. Special thanks go to Mr. Michal Hanus. Some experiments were carried out at the Department of Technical Education, University Hradec Králové and other experiments at the Faculty of Transportation CVUT.

REFERENCES

[1] H.O. Fuchs, R.L. Stephens, *Metal fatigue in engineering*, John Wiley & Sons, Pub., 1980.

[2] Y. Murakami, *Metal Fatigue: Effects of small defects and nonmetallic inclusions*, Elsevier, 2002.

[3] D.F. Socie, G.B. Marquis, *Multiaxial fatigue.* Warrendale, 2000.

[4] F. Ellyin, *Fatigue Damage, Crack Growth and Life Prediction*, Chapman & Hall 1997.

[5] F. Ellyin, Z. Xia, "A general fatigue theory and its applications to out-of-phase cyclic loading", *Journal of Engng. Mater. Technol.*, Transactions of the ASME, 115, 1993, pp. 411-416.

[6] J.A. Bannantine, D.F. Socie, "A multiaxial fatigue life estimation technique", *Advances in Fatigue Lifetime Predictive Techniques*, ASTM STP 1122. Eds: M. R. Mitchell a R. W. Landgraf. Philadelphia, American society for testing and materials 1992, pp. 249-275.

[7] J.M. Ayllón, C. Navarro, J. Vázquez, J. Domínguez, "Fatigue life estimation in dental implants" *Engineering Fracture Mechanics* 123 (2014) pp. 34–43

[8] S. Major S, V. Kocour, P. Cyrus P, "Fatigue life prediction of pedicle screw for spinal Surgery", *Frattura ed Integrita Strutturale*, 10 (35), 2016 , pp. 379-388

[9] S. Major, V. Kocour, S. Hubálovský, "Fatigue testing and calculation of a conical pedicle screws for spine fusion", Ed. P. Padevět, P. Bittnar, *EAN 2015 - 53rd Conference on Experimental Stress Analysis*. Praha: Czech Technical University in Prague, 2015, s. 229-232.

[10] L. Gajdoš, M. Šperl, J. Frankl. J. Kaiser, V. Mentl., J. Kyncl, J. Lukeš, R. Kužel, "Verification of trend MPL variation in fatigue by modern methods", Key Engineering Materials 606, 2014 pp. 99-102.

[11] L. Gajdoš, M. Šperl, J. Bystrianský, Fatigue behaviour of X70 steel in crude oil, Materials and Technology. 2015, roč. 49, č. 2, s. 243-246, 2015,

[12] M. Hoffmann; T. Seeger, "A Generalized Method for Estimating Multiaxial Elastic-Plastic Notch Stresses and Strains, Part I & II." . *J. of Engng. Mater. & Technology*, Vol. 107, 1985, pp. 250-260.

[13] A. Carpinteri, E. Macha, R. Brighenti, A. Spagnoli, "Expected principal stress directions under multiaxial random loading. Part I: theoretical aspects of the weight function method.", *Int. J. Fatigue* 21, 1999, pp. 83-88.

[14] M.W. Brown, D.K. Suker, C.H. Wang, "An analysis of mean stress in multiaxial random fatigue", *Fatigue Fract. Engng. Mater. Struct.* 19, 1996, No. 2/3, pp. 323-333.

[15] L. Gajdoš, M. Šperl, Critical conditions of pressurized pipes, Engineering Mechanics. 2013, roč. 20, č. 5, s. 401-412, 2013

[16] S. Major, P. Cyrus, M. Hubálovská, "The Influence of surface roughness on biocompatibility and fatigue life of titanium based alloys"**,** *IOP Conf. Series: Materials Science and Engineering* 175, 2017, pp. 1-5

[17] S. Hosseini, "Fatigue of Ti-6Al-4V", *Biomedical engineering - technical applications in medicine*, Dr. Radovan Hudak (Ed.), 2012, pp.75-92.

[18] ASTM E647-08, *Standard Test Method for Measurement of Fatigue Crack Growth Rates*, ASTM International, West Conshohocken, PA, 2008

[19] M. Kulkani, A. Mazare, P. Schmuki, A. Iglic. "Biomaterial surface modification of titanium and Titanium Alloys for Medical Applications", *Nanomedicine*, One Central Press, Ed: Alexander Seifalian, Achala de Mel, Deepak M. Kalaskar, 2014, pp.111-136

[20] A. Anders, "*Handbook of plasma immersion ion implantation and deposition*", New York: John Wiley & Sons, 2000, pp. 111-136.

[21] S. Major, J. Papuga, J. Horníková, J.Pokluda, "Comparison of fatigue criteria for combined bending-torsion loading of nitrided and virgin specimens", *Strength of Materials* 40, No.1 (2008), pp. 73-76.

[22] S. Major, S. Hubálovský, V. Kocour, J.Valach, "Effectiveness of the Modified Fatigue Criteria for Biaxial Loading Notched Specimen in High-Cycle Region", *Applied mechanics and Materials* Vol.732, 2015, pp. 63-70.

[23] I.V. Papadopoulos, P. Davoli, P. Gorla, M. Filippiny, A. Bernasconi, "A comparative study of multiaxial high-cycle fatigue criteria for metals", *Int. J. Fatigue* 19, No. 3, 1997, pp. 219-235.

[24] H. J. Gough, H. V. Pollard, W. J. Clenshaw, *Some experiments on the resistance of metals to fatigue under combined stresses*, London, His Majesty's Stationery Office 1951.

[25] H. J. Gough, "Engineering steels under combined cyclic and static Stresses", *Journal of Applied Mechanics*, June 1950, pp. 113-125.

[26] A.A. Ilyushin, *Plasticity Foundations of General Mathematical Theory*, Akad. Nauk, Moscow, 1963, p. 16.

[27] D. L. McDiarmid, "Fatigue under out-of-phase bending and torsion. Fatigue Fract", *Engng. Mater. Struct.*, 9, 1987, pp. 457-475.

[28] D. L. McDiarmid, "A general criterion for high cycle multiaxial fatigue failure", *Fatigue Fract. Engng. Mater. Struct.*, 14, 1991, No. 4, pp. 429-453.

[29] D. L. McDiarmid, "A shear stress based critical-plane criterion of multiaxial fatigue failure for design and life prediction", *Fatigue Fract. Engng. Mater. Struct* 17, 1994, No. 12, pp. 1475-1484.

[30] G. Sines, "Behavior of metals under complex static and alternating stresses", Metal Fatigue. Red. G. Sines a J.L. Waisman, New York, McGraw Hill 1959, pp. 145-469.

[31] W. N. Findley, "Fatigue of metals under combinations of stresses", *Transactions of ASME* (vol. 79), 1957.

[32] B. Crossland, "Effect of large hydrostatic pressure on the torsional fatigue strength of an alloy steel", *Proc. Int. Conf. on Fatigue of Metals*, Institution of Mechanical Engineers, London, 1956, pp. 138-149.

[33] A. Carpinteri, A.Spagnoli, "Multiaxial high-cycle fatigue criterion for hard metals", *Int. J. Fatigue* 23, 2001, pp. 135-145

[34] I.V. Papadopoulos, "A new criterion fatigue strenght for out-of-phase bending and torsion of hard metals", *Int. J. Fatigue* 16, 1994, pp. 377-384.

[35] I.V. Papadopoulos, "Fatigue limit of metals under multiaxial stress conditions: the microscopic approach". Technical note no. I.93.101. Commission of the European Communities, Joint Research Centre, ISEI/IE 2495/93, 1993.

[36] I.V. Papadopoulos, "Critical plane approaches in high-cycle fatigue", *Fatigue Fracture Engng. Mater. Struct.* 21 No. 3, 1998, pp. 269-285.

[37] D.L .McDiarmid, "A general criterion for high cycle multiaxial fatigue failure", *Fatigue Fracture Engng. Mater. Struct.* 14, No. 4, 1991, pp. 429-453.

[38] D. L .McDiarmid, "A shear stress based critical-plane criterion of multiaxial fatigue failure for design and life prediction", *Fatigue Fracture Engng. Mater. Struct.* 17, No. 12, 1994, pp. 1475-1484.

[39] K. Dang Van, G. Cailletaud, J. F. Flavenot, L. Douaron, H.P. Liuerade, "Criterion for high-cycle failure under multiaxial loading", *Biaxial and Multiaxial Fatigue*, Eds: M. Brown and K. Miller, Sheffield, 1989, pp. 459-478.

[40] J. L. Kenmeugne, E. Vidal-Salle, J.L. Robert, R.J. Bahuaud, "On a new multiaxial fatigue criterion based on a selective integration approach", Fatigue 96, *Proc. of the sixth Int. Fatigue Congress*, Vol. II. Red. G. Lutjering, Berlin, Pergamon 1996, pp. 1013-1018.

[41] C.A. Gonçalves, J.A. Araujo, E.N. Mamaya, Multiaxial fatigue*:* "A stress based criterion for hard metals", *Int. J. Fatigue* 27, 2005, pp. 177-187.

[42] L. Reis, B. Li, M. De Freitas, "Biaxial fatigue for proportional and non-proportional loading path", *Fatigue Fract. Engng. Mater. Struct.* 27, 2004, pp. 775-784.

[43] H. Zenner, A. Simburger, A.; J.LIU, "On the fatigue limit of ductile metals under complex multiaxial loading", *Int. Journal of Fatigue* 22, 2000, pp. 137-145.

[44] H. Zenner, R. Heidenreich, I. Z. Richter, "Fatigue strength under nonsynchronous multiaxial stresses", *Mat. Wiss und Werkstofftech* 16, 1985, p. 101-112.

[45] J. Liu, H. Zenner, "Berechnung der Dauerschwingfestigkeit bei mehrachsiger Beanspruchung", *Mat. Wiss und Werkstofftech* 24(S), 1993, pp. 240–249.

[46] J. Papuga, "Mapping of Fatigue Damages", PhD Thesis, CTU Prague, Czech republic, 2005.